Shotgun analysis of rough-type lipopolysaccharides using ultraviolet photodissociation mass spectrometry

Dustin R. Klein, Dustin D. Holden, Jennifer S. Brodbelt

Department of Chemistry
The University of Texas at Austin
1 University Station A5300
Austin, TX 78712, USA

Supporting Information: The contents of the supporting information include figures showing the modified Orbitrap mass spectrometer, examples of ESI mass spectra of *E. coli* LPS, carbohydrate fragmentation nomenclature, an energy-variable CID diagram of penta-acylated LPS, a CID-CID mass spectrum of tetra-acylated LPS, CID spectra of two isobaric LPS, CID-HCD and CID-UVPD mass spectra of two isobaric LPS, and tables of identified fragment ions.

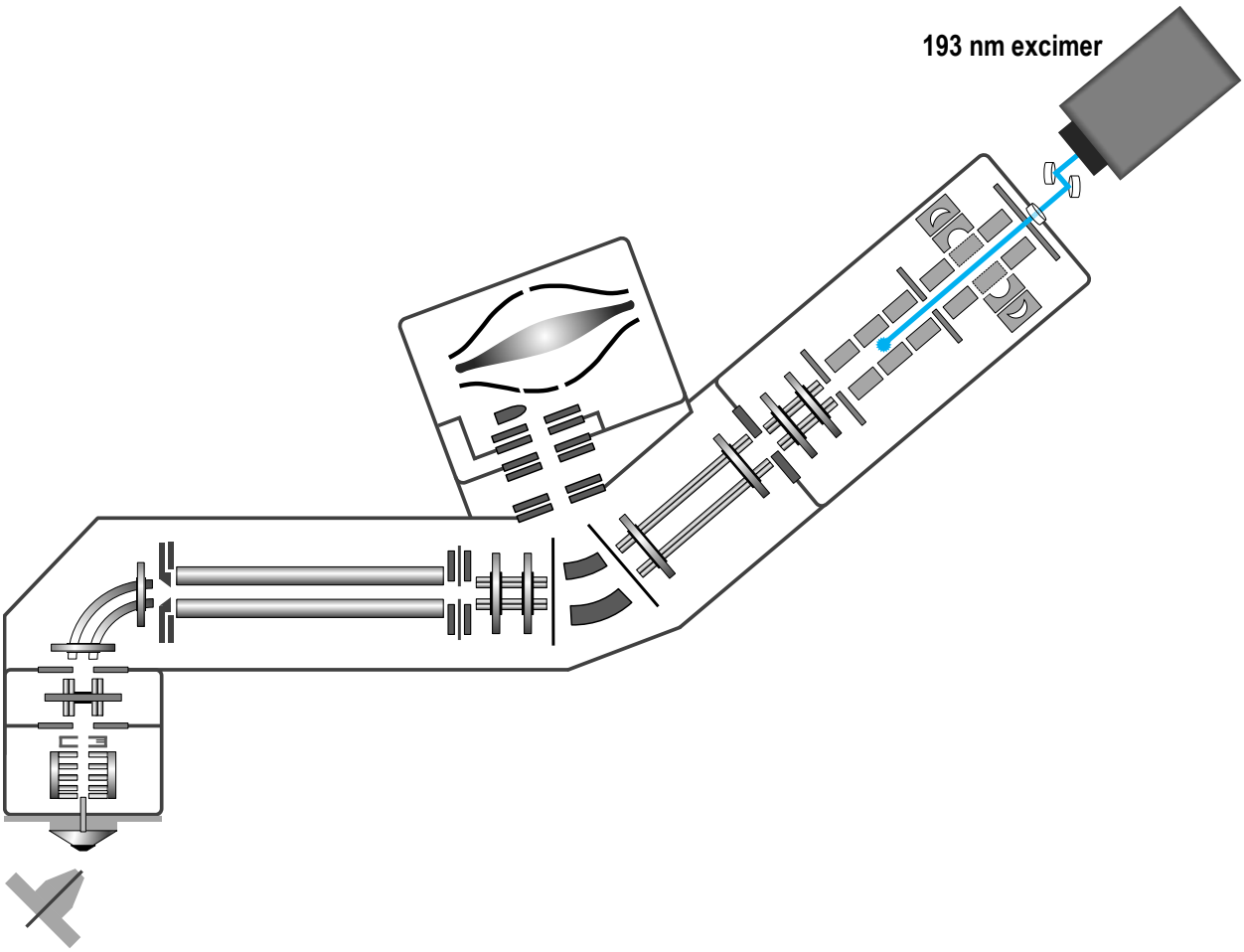

Figure S1. Schematic of a Thermo Orbitrap Fusion modified with a 193 nm excimer laser.

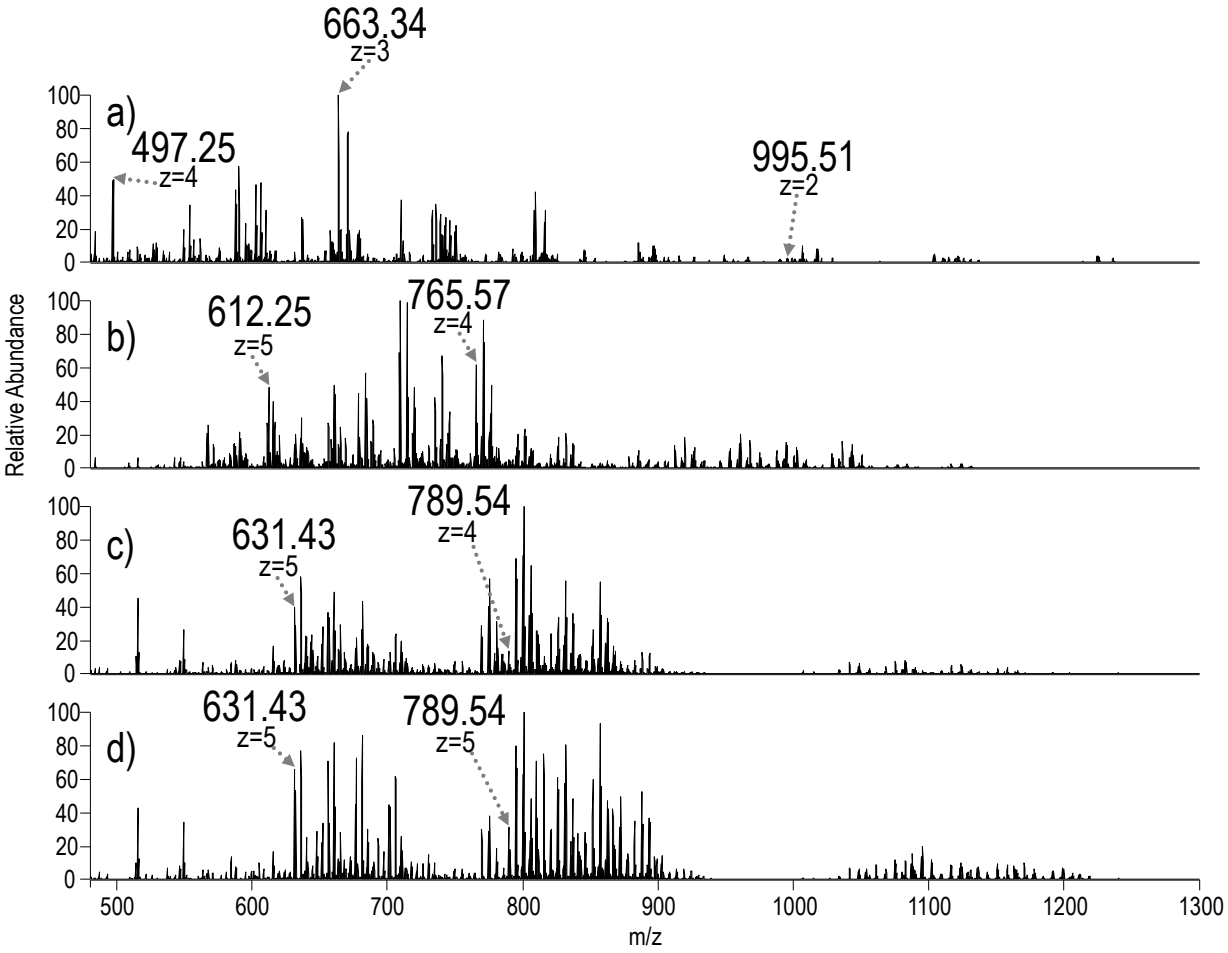

Figure S2. ESI mass spectra (100 ug/mL) of a) *S. enterica* Rd1, b) *S. enterica* Rb, c) *E. coli* R2 and d) *E. coli* R3 infused without chromatographic separation into the mass spectrometer via static emitters.

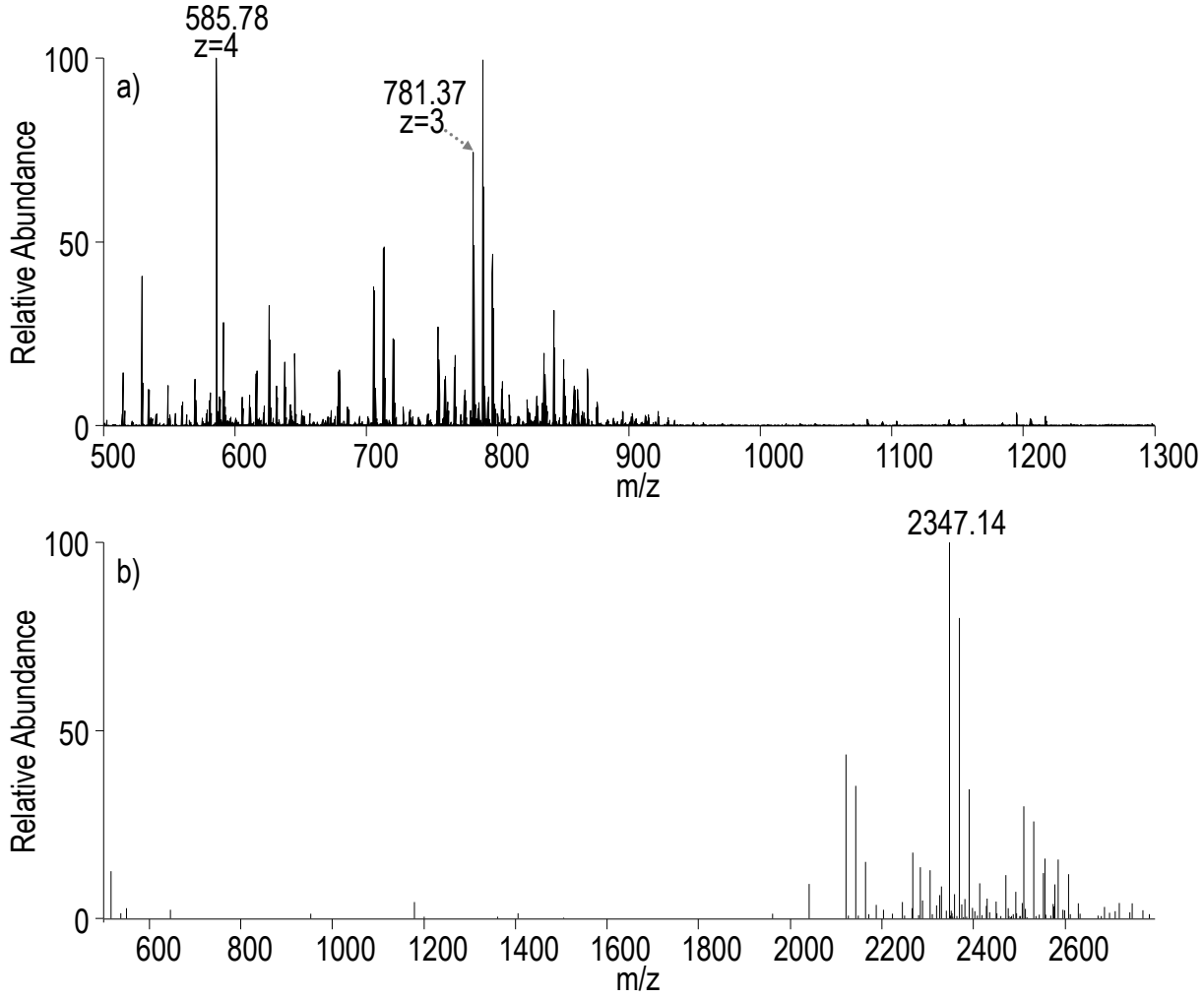

Figure S3. a) ESI mass spectrum of *S. enterica* Rc (100 ug/mL) infused without chromatographic separation into the mass spectrometer via a static emitter, and b) deconvoluted spectrum.

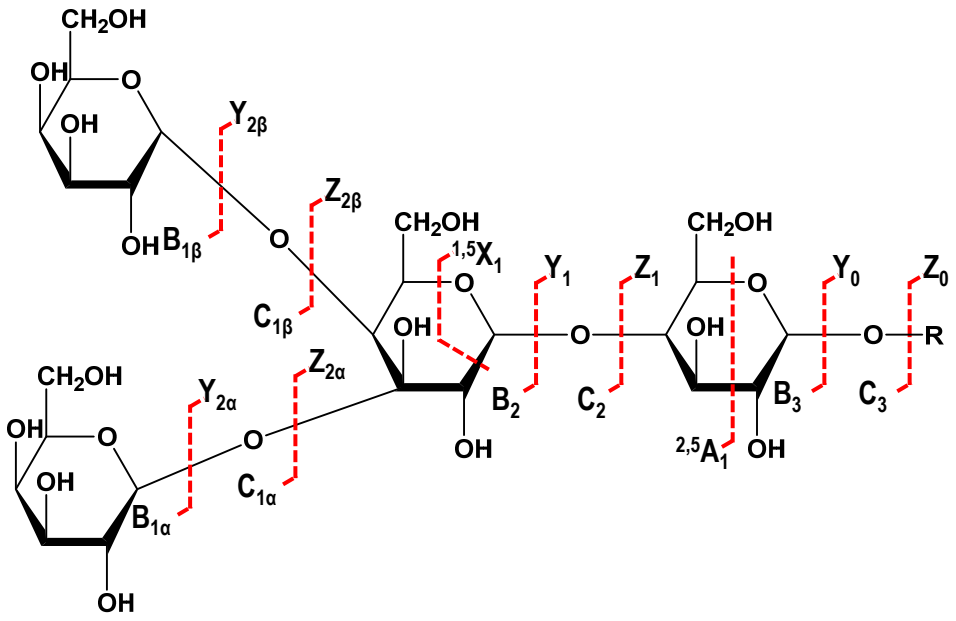

Figure S4. Domon and Costello carbohydrate fragmentation nomenclature (Reference 41)

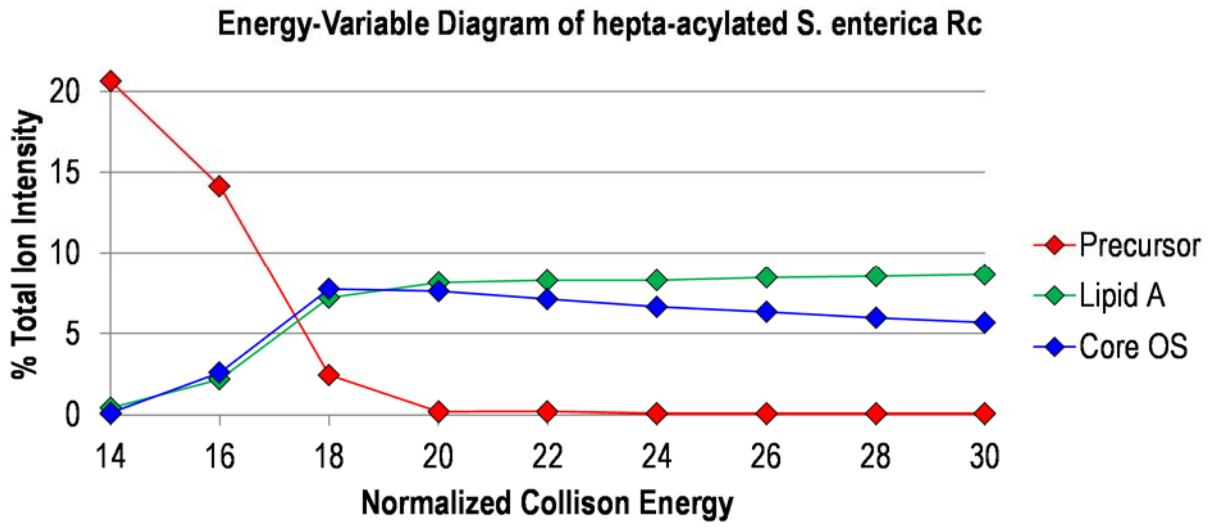

Figure S5. CID energy-variable diagram of penta-acylated S. enterica Rc monitoring the precursor ion (m/z 642.57) and products ions corresponding to the oligosaccharide substructure (m/z 492.14) and lipid A substructure (m/z 792.5).

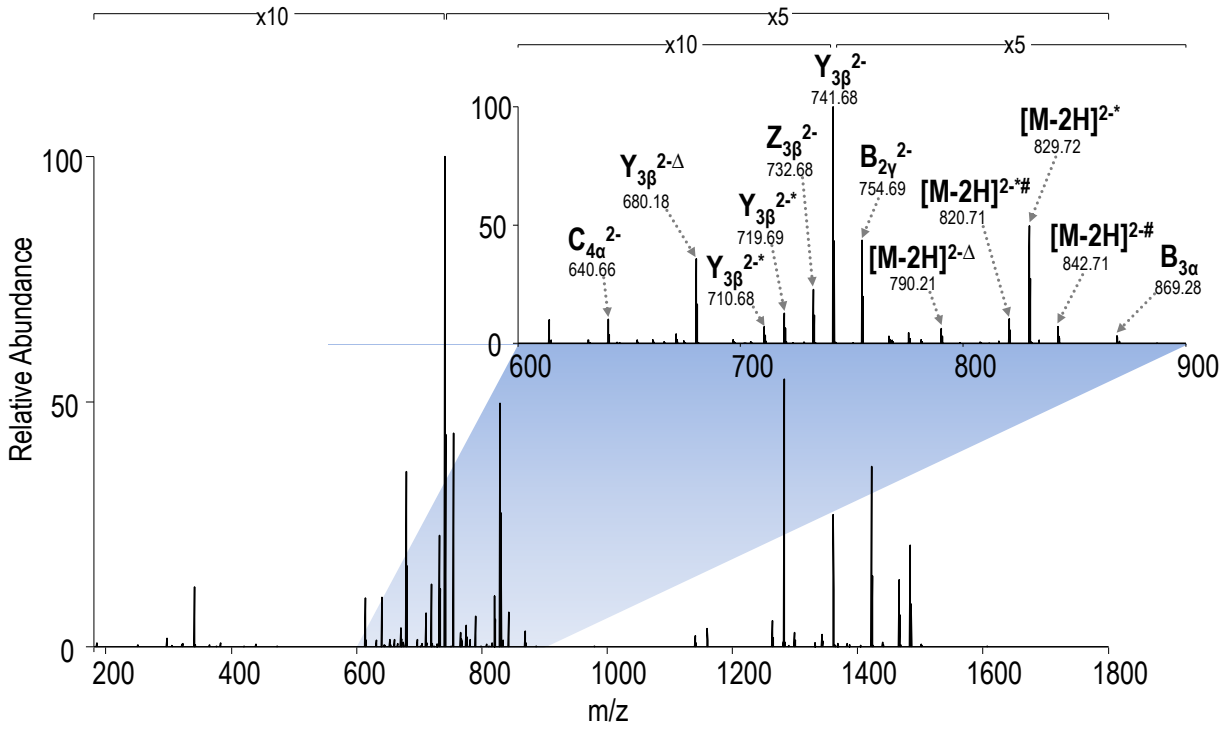

Figure S6. CID-CID mass spectrum (NCE 18- NCE 30) of the core oligosaccharide substructure of tetra-acylated *S. enterica* Rb containing a pyrophosphoethanolamine modification (m/z 851.81). The inset shows expansion of the range from m/z 600 to 900. Δ = loss of phosphethanolamine; * = loss of CO_2; # = loss of H_2O

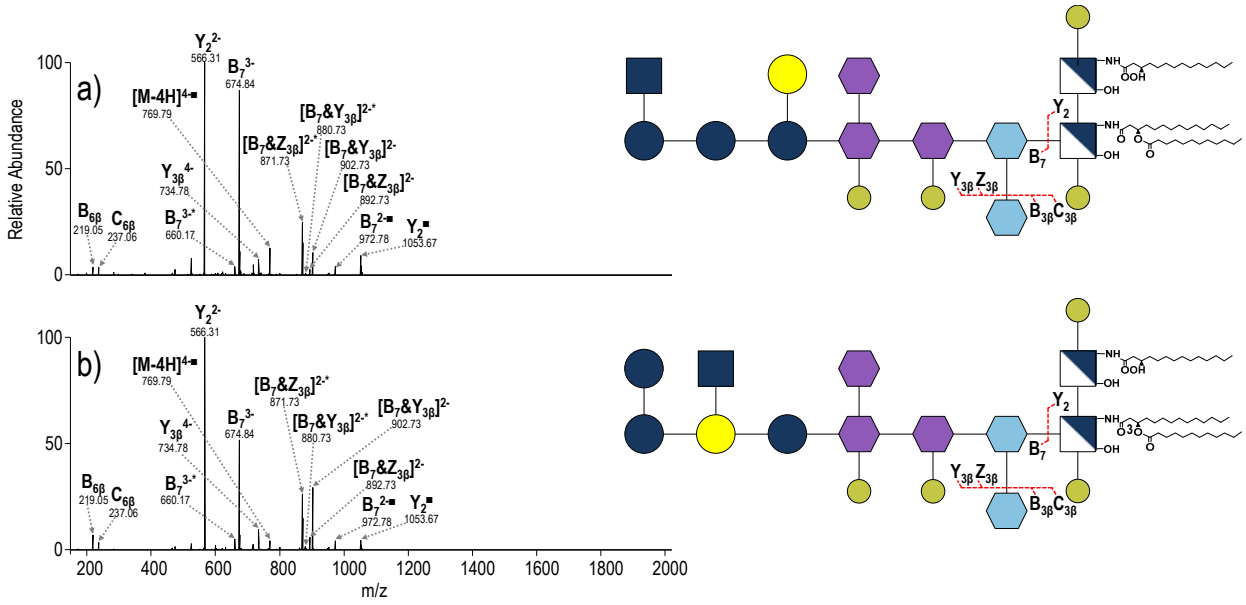

Figure S7. a) CID (NCE 18) of *E. coli* R2 (MW = 3162.16 Da, precursor m/z 631.43, charge state 5-) b) CID (NCE 18) of *E. coli* R3 (MW = 3162.16 Da, precursor m/z 631.43, charge state 5-); ■= neutral loss of HPO_3; & indicates that both of the indicated cleavages occur to generated a particular fragment ion.

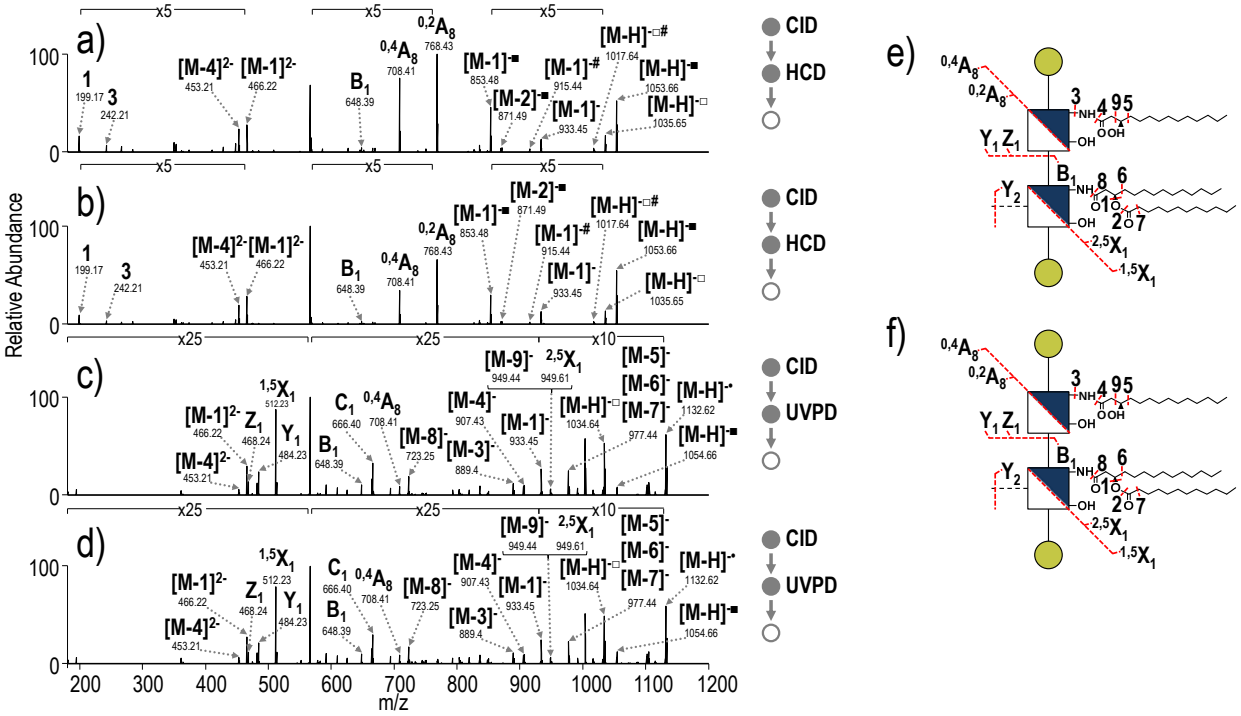

Figure S8. a) CID-HCD (NCE 18- NCE 30) of the lipid A substructure of *E. coli* R2 (m/z 566.31, charge state 2-) b) CID-HCD (NCE 18- NCE 30) of the lipid A substructure of *E. coli* R3 (m/z 566.31, charge state 2-), c) CID-UVPD (NCE 18- 5 pulses, 2 mJ) of the lipid A substructure substructure of *E. coli* R2 (m/z 566.31, charge state 2-) and d) CID-UVPD (NCE 18- 5 pulses, 2 mJ) of the lipid A substructure of *E. coli* R3 (m/z 566.31, charge state 2-). ■= neutral loss of HPO_3, □= neutral loss of HPO_3, #= neutral loss of H_2O. A bracket under a pair of ions indicates the presence of two resolved ions, but the mass difference is too small to allow inclusion of separate arrows. The acyl chains are numbered, and the loss of a particular acyl chain is denoted as M – N where M represents the LPS and N represents the acyl chain that is lost.

Table S1. List of identified ions in Figure 4

Figure 4a	
m/z	Fragment
1484.37	$Y_{3\beta}$
1466.36	$Z_{3\beta}$
1440.38	$Y_{3\beta}^{*}$
1422.37	$Z_{3\beta}^{*}$
1361.36	$Y_{3\beta}^{\Delta}$
1343.35	$Z_{3\beta}^{\Delta}$
1282.32	$C_{4\alpha}$
1264.31	$B_{4\alpha}$
1159.32	$C_{4\alpha}^{\Delta}$
1141.31	$B_{4\alpha}^{\Delta}$
869.28	$B_{3\alpha}$
842.71	$[M-2H]^{2-\#}$
829.72	$[M-2H]^{2-*}$
820.71	$[M-2H]^{2-\#*}$
790.21	$[M-2H]^{2-\Delta}$
754.69	$B_{2\gamma}^{2-}$
741.68	$Y_{3\beta}^{2-}$
732.68	$Z_{3\beta}^{2-}$
719.69	$Y_{3\beta}^{2-*}$
710.68	$Z_{3\beta}^{2-*}$
680.18	$Y_{3\beta}^{2-\Delta}$
640.66	$C_{4\alpha}^{2-}$
421.10	$Y_{3\alpha}^{*}$
377.11	$Z_{3\alpha}^{*}$

Figure 4b	
m/z	Fragment
1501.45	$[M-▼]^{-}$
1484.37	$Y_{3\beta}$
1466.36	$Z_{3\beta}$
1440.38	$Y_{3\beta}^{*}$
1422.37	$Z_{3\beta}^{*}$
1361.36	$Y_{3\beta}^{\Delta}$
1343.35	$Z_{3\beta}^{\Delta}$
1282.32	$C_{4\alpha}$
1264.31	$B_{4\alpha}$
1159.32	$C_{4\alpha}^{\Delta}$
1141.31	$B_{4\alpha}^{\Delta}$
1123.29	$B_{4\alpha}^{\Delta\#}$
967.25	$[C_{4\alpha}\&Y_{5\gamma}]^{\Delta}$
869.28	$B_{3\alpha}$
851.71	$B_{5\alpha}$
842.71	$[M-2H]^{2-\#}$
829.72	$[M-2H]^{2-*}$
820.71	$[M-2H]^{2-\#*}$
790.21	$[M-2H]^{2-\Delta}$
754.69	$B_{2\gamma}^{2-}$
741.68	$Y_{3\beta}^{2-}$
732.68	$Z_{3\beta}^{2-}$
719.69	$Y_{3\beta}^{2-*}$
710.68	$Z_{3\beta}^{2-*}$
680.18	$Y_{3\beta}^{2-\Delta}$
640.66	$C_{4\alpha}^{2-}$
439.11	$Y_{3\alpha}$
421.10	$Y_{3\alpha}^{*}$
377.11	$Z_{3\alpha}^{*}$
237.06	$C_{4\beta}$
219.98	▼
219.05	$B_{4\beta}$
201.04	$B_{4\beta}^{\#}$

Figure 4c	
m/z	Fragment
1703.42	$[M-H]^{\cdot-}$
1685.41	$[M-H]^{\cdot-\#}$
1673.41	$[M-CH_3O]^{\cdot-\#}$
1661.39	$[M-C_2H_6N]^{\cdot-}$
1630.39	$^{3,5}X_{6\alpha}$, $^{3,5}X_{6\delta}$
1601.39	$^{2,5}X_{6\alpha}$, $^{2,5}X_{6\delta}$
1570.37	$^{1,5}X_{6\alpha}$, $^{1,5}X_{6\delta}$
1540.36	$Y_{6\alpha}$, $Y_{6\delta}$
1525.37	$Z_{6\alpha}$, $Z_{6\delta}$
1512.37	$Y_{5\gamma}$
1467.37	$Z_{3\beta}$
1422.37	$Z_{3\beta}^{*}$
1282.32	$C_{4\beta}^{*}$
1263.31	$B_{4\beta}$
1246.27	$^{1,5}X_{5\alpha}$
1218.27	$Y_{5\alpha}$
1200.26	$Z_{5\alpha}$
862.15	$^{1,5}X_{4\alpha}$
851.71	B_5
842.20	$[M-2H]^{2-\cdot\#}$
829.21	$[M-C_2H_6N]^{2-}$
799.69	$^{2,5}X_{6\alpha}^{2-}$, $^{2,5}X_{6\delta}^{2-}$
770.68	$Y_{6\alpha}^{2-}$,$Y_{6\delta}^{2-}$
762.18	$Z_{6\alpha}^{2-}$,$Z_{6\delta}^{2-}$
755.68	$Y_{5\gamma}^{2-}$
741.68	$Y_{3\beta}^{2-}$
733.68	$Z_{3\beta}^{2-}$
640.66	$C_{4\alpha}^{2-}$

Figure 4d	
m/z	Fragment
1279.85	$[M-H]^{-■}$
1261.84	$[M-H]^{-□}$
1159.64	$[M-3]^{-}$
1115.61	$[M-1]^{-}$
1095.67	$[M-4]^{-■}$
1079.67	$[M-3]^{-■}$
1035.65	$[M-1]^{-■}$, $[M-2]^{-□}$, $[M-5]^{-□}$
994.62	$^{1,3}A_7$
915.44	$[M-1-3]^{-}$
708.41	Y_1
670.40	Z_2^{2-}
587.31	$[M-4]^{2-}$
579.32	$[M-3]^{2-}$
566.31	$[M-2]^{2-}$, $[M-5]^{2-}$
557.30	$[M-1]^{2-}$
466.22	$[M-2-3]^{2-}$, $[M-1-4]^{2-}$
457.21	$[M-1-3]^{2-}$
444.21	$[M-1-5]^{2-}$
243.20	1
199.19	3

Figure 4e	
m/z	Fragment
1279.85	$[M-H]^{-■}$
1261.84	$[M-H]^{-□}$
1159.64	$[M-3]^{-}$
1115.61	$[M-1]^{-}$
1095.67	$[M-4]^{-■}$
1079.67	$[M-3]^{-■}$
1035.65	$[M-1]^{-■}$, $[M-2]^{-□}$, $[M-5]^{-□}$
994.62	$^{1,3}A_7$
915.44	$[M-1-3]^{-}$
708.41	Y_1
664.38	C_6
587.31	$[M-4]^{2-}$
579.32	$[M-3]^{2-}$
566.31	$[M-2]^{2-}$, $[M-5]^{2-}$
557.30	$[M-1]^{2-}$
466.22	$[M-2-3]^{2-}$, $[M-1-4]^{2-}$
457.21	$[M-1-3]^{2-}$
448.21	$[M-1-3]^{2-\#}$
444.21	$[M-1-5]^{2-}$
243.20	1
242.21	10
199.19	3

Figure 4f	
m/z	Fragment
1358.81	$[M-H]^{\cdot-}$
1298.79	$^{0,4}X_1$
1203.63	$[M-7]^{\cdot-}$,$[M-9]^{\cdot-}$
1175.80	$^{2,5}X_1$
1174.63	$[M-6]^{\cdot-}$,$[M-8]^{\cdot-}$
1159.81	$^{0,2}X_1$
1159.64	$[M-3]^{-}$
949.44	$[M-11]^{-}$
920.42	$^{1,2}X_1$
892.42	$^{1,3}X_1$
874.41	$[M-1-10]^{-}$
817.38	$^{1,4}A_7$
738.42	$^{1,5}X_1$
710.42	Y_1
692.41	Z_1
664.38	C_6
587.31	$[M-4]^{2-}$
579.32	$[M-3]^{2-}$
566.31	$[M-2]^{-}$,$[M-5]^{-}$
474.22	$[M-2-4]^{2-}$
466.22	$[M-2-3]^{2-}$, $[M-1-4]^{2-}$
243.20	1

Table S2. List of identified ions in Figure 5

Figure 5a	
m/z	**Fragment**
1585.00	$[M-H]^{\bullet-}$
1506.05	$[M-H]^{\bullet\blacksquare-}$
1487.03	$[M-H]^{\bullet\square-}$
1429.82	$[M-7]^{\bullet-}$, $[M-10]^{\bullet-}$, $[M-13]^{\bullet-}$
1400.82	$[M-6]^{\bullet-}$, $[M-8]^{\bullet-}$, $[M-9]^{\bullet-}$
1385.83	$[M-5]^{-}$
1340.80	$[M-1]^{\bullet-}$, $[M-3]^{\bullet-}$
1158.64	$[M-14]^{\bullet-}$
890.58	C_1
738.42	$^{1,5}X_1$
710.43	Y_1
692.42	$[M-5]^{2-}$
679.41	$[M-2]^{2-}$, $[M-4]^{2-}$, $[M-11]^{2-}$
243.20	1,3

Figure 5b	
m/z	**Fragment**
1585.00	$[M-H]^{\bullet-}$
1506.05	$[M-H]^{\bullet\blacksquare-}$
1487.03	$[M-H]^{\bullet\square-}$
1429.82	$[M-7]^{\bullet-}$, $[M-10]^{\bullet-}$, $[M-13]^{\bullet-}$
1400.82	$[M-6]^{\bullet-}$, $[M-8]^{\bullet-}$, $[M-9]^{\bullet-}$
1385.83	$[M-5]^{-}$
1340.80	$[M-1]^{\bullet-}$, $[M-3]^{\bullet-}$
1158.64	$[M-14]^{\bullet-}$
890.58	C_1
738.42	$^{1,5}X_1$
710.43	Y_1
692.42	$[M-5]^{2-}$
679.41	$[M-2]^{2-}$, $[M-4]^{2-}$, $[M-11]^{2-}$
243.20	1,3

Table S3. List of identified ions in Figure 6

Figure 6a	
m/z	Fragment
1726.50	$Y_{3\beta}^{\blacksquare}$
1708.49	$Z_{3\beta}^{\blacksquare}$
1524.45	$C_{6\alpha}^{\blacksquare}$
1506.44	$B_{6\alpha}^{\blacksquare}$
1412.35	$B_{6\alpha}$&$Y_{5\gamma}$
1332.38	$C_{5\alpha}$
1314.37	$B_{5\alpha}$
972.77	$[M-2H]^{2-\blacksquare}$
902.73	$Y_{3\beta}^{2-}$
893.72	$Z_{3\beta}^{2-}$
801.70	$C_{6\alpha}^{2-}$
792.70	$B_{6\alpha}^{2-}$
601.48	$Y_{3\beta}^{3-}$
526.18	$B_{3\alpha}$
491.08	$Y_{3\beta}$&$Y_{4\alpha}$
424.15	$^{2,4}A_{3\alpha}$
237.06	$C_{6\beta}$
219.05	$B_{6\beta}$

Figure 6b	
m/z	Fragment
1726.50	$Y_{3\beta}^{\blacksquare}$
1708.49	$Z_{3\beta}^{\blacksquare}$
1524.45	$C_{6\alpha}^{\blacksquare}$
1506.44	$B_{6\alpha}^{\blacksquare}$
1412.35	$B_{6\alpha}$&$Y_{5\gamma}$
1332.38	$C_{5\alpha}$
1314.37	$B_{5\alpha}$
972.77	$[M-2H]^{2-\blacksquare}$
902.73	$Y_{3\beta}^{2-}$
893.72	$Z_{3\beta}^{2-}$
801.70	$C_{6\alpha}^{2-}$
792.70	$B_{6\alpha}^{2-}$
601.48	$Y_{3\beta}^{3-}$
491.08	$Y_{3\beta}$&$Y_{4\alpha}$
341.11	$C_{2\alpha}$
323.10	$B_{2\alpha}$
237.06	$C_{6\beta}$
219.05	$B_{6\beta}$

Figure 6c	
m/z	Fragment
1980.51	$[M-H]^{-*}$
1863.46	$Y_{6\delta}$
1823.44	$Y_{8\alpha}$
1788.45	$Z_{3\beta}$
1661.39	$Y_{7\alpha}$
1643.48	$Z_{7\alpha}$
1604.42	$C_{6\alpha}$
1585.39	$B_{6\alpha}$
1399.32	$^{2,4}X_{5\alpha}$
1330.37	$C_{5\alpha}^{\bullet}$
1313.37	$B_{5\alpha}^{\bullet}$
1012.25	$[M-2H]^{2-\bullet}$
931.73	$Y_{6\delta}^{2-}$
922.72	$Z_{6\delta}^{2-}$
911.22	$Y_{8\alpha}^{2-}$
902.73	$Z_{3\beta}^{2-}$
894.23	$Y_{3\beta}^{2-}$
844.19	$^{1,5}X_{7\alpha}^{2-}$
830.19	$Y_{7\alpha}^{2-}$
821.19	$Z_{7\alpha}^{2-}$
740.16	$Z_{6\alpha}^{2-}$
711.14	$Y_{4\alpha}$
695.15	$Z_{4\alpha}$
439.11	$Y_{3\alpha}$
237.06	$C_{6\beta}$

Figure 6d	
m/z	Fragment
1980.51	$[M-H]^{-*}$
1788.45	$Z_{3\beta}$
1702.42	$Y_{7\alpha}$
1684.41	$Z_{7\alpha}$
1604.42	$C_{6\alpha}$
1585.39	$B_{6\alpha}$
1332.39	$C_{5\alpha}$
1321.29	$Z_{6\alpha}$
1313.37	$B_{5\alpha}^{\bullet}$
1175.23	$Y_{5\alpha}$
1159.24	$Z_{5\alpha}$
1012.25	$[M-2H]^{2-\bullet}$
931.73	$Y_{8\alpha}^{2-}$
922.72	$Z_{8\alpha}^{2-}$
910.22	$Y_{7\delta}^{2-}$
902.73	$Z_{3\beta}^{2-}$
894.23	$Y_{3\beta}^{2-}$
841.7	$Z_{7\alpha}^{2-}$
711.14	$Y_{4\alpha}$
682.14	$^{1,5}X_{6\alpha}$
439.11	$Y_{3\alpha}$
237.06	$C_{6\beta}$
219.05	$B_{6\beta}$